ISSN 1067-8212, Russian Journal of Non-Ferrous Metals, 2017, Vol. 58, No. 6, pp. 632–638. © Allerton Press, Inc., 2017.

PRESSURE TREATMENT OF METALS

A Study of Plastic Deformation Behavior of AA1050 Aluminum Alloy during Pure Shear Extrusion with Back Pressure[1]

Missam Irani[a] and Mansoo Joun[b, *]

[a] *Graduate School of Mechanical and Aerospace Engineering, Gyeongsang National University, Jinju-City, 664-953 Republic of Korea*

[b] *Engineering Research Institute, School of Mechanical and Aerospace Engineering, Gyeongsang National University, Jinju-City, 664-953 Republic of Korea*

**e-mail: msjoun@gnu.ac.kr*

Received June 4, 2017

Abstract—In the present study, the effects of back pressure on the filling fraction of die and the effective strain distribution throughout severely deformed material during pure shear extrusion, a novel severe plastic deformation process, are investigated by finite element analysis. A pure shear extrusion process found in the literature is employed and the predicted forming load is compared with experiments. A good agreement is observed between the results of the simulation with Coulomb friction of 0.12 and experiments. Various back pressures are applied to plunger at the exit channel of the die, and their influence on the filling fraction of the die and the effective strain in severely deformed billets are studied, indicating that the homogeneity of the effective strain on the cross-section of the deformed billet is decreased slightly. It is also found that the filling fraction of the die exit channel as well as average strain on the cross-section of the billet are increased.

Keywords: pure shear extrusion, finite element method, strain homogeneity, back pressure, filling fraction

DOI: 10.3103/S1067821217060049

1. INTRODUCTION

Severe plastic deformation (SPD) can be induced in metals by a number of metal working techniques, including high pressure torsion (HTP), accumulative roll bonding (ARB), equal channel angular pressing (ECAP), pure shear extrusion (PSE) and the like, and they are able to reduce grain size to submicron dimensions [1]. The common feature of these processes is high strain imposed without significant change of the overall dimensions of workpiece which requires repetition of the deformation process to accumulate plastic deformation, leading to create of nanostructures. This makes it possible to repeat the deformation processes so that plastic deformations can be accumulated, in order to create nanostructures [2]. Thus, the repeatability of a SPD process is a key factor of determining its effectiveness. However, while the entrance and exit channel cross-sections are the same in ECAP, HPT, PSE and the like, the cross section of a severely deformed material is not completely the same as the initial one due to the incomplete filling of the die [3, 4].

The homogeneity of strain induced by a SPD process is a significant factor which dominates the uniformity of the mechanical properties of the deformed material. Most existing SPD methods impose an inhomogeneous strain in the processed material, which may cause unfavorable microstructural inhomogeneity and poor overall mechanical properties of the products [5–7]. Recently, great efforts of metallurgical experiments and finite element methods have been devoted to investigating into the homogeneity of SPD processed bulk materials [8]. These studies revealed that back pressure in a SPD process contributes to an increase in the magnitude of the induced strain on the cross-section of the deformed material [9–11]. However, its effects on homogeneity of strain is not similar in different SPD processes. For example in twist extrusion, the homogeneity of strain improves when the back pressure is applied, while in simple shear extrusion homogeneity is reduced by applying back pressure [12]. It is generally known that back pressure not only applies higher hydrostatic pressure and more deformation compared to a regular SPD, but it also prevents surface defects of the material [13]. Many other advantages of imposing back pressure during a SPD process have been reported, including an improvement in mechanical properties and decrease in internal void initiation. It has been known that the enhancement of mechanical properties is owing to the accelerated refinement of microstructure in the presence of back pressure [14–16]. Employing back pressure in a SPD method also leads to an

[1] The article is published in the original.

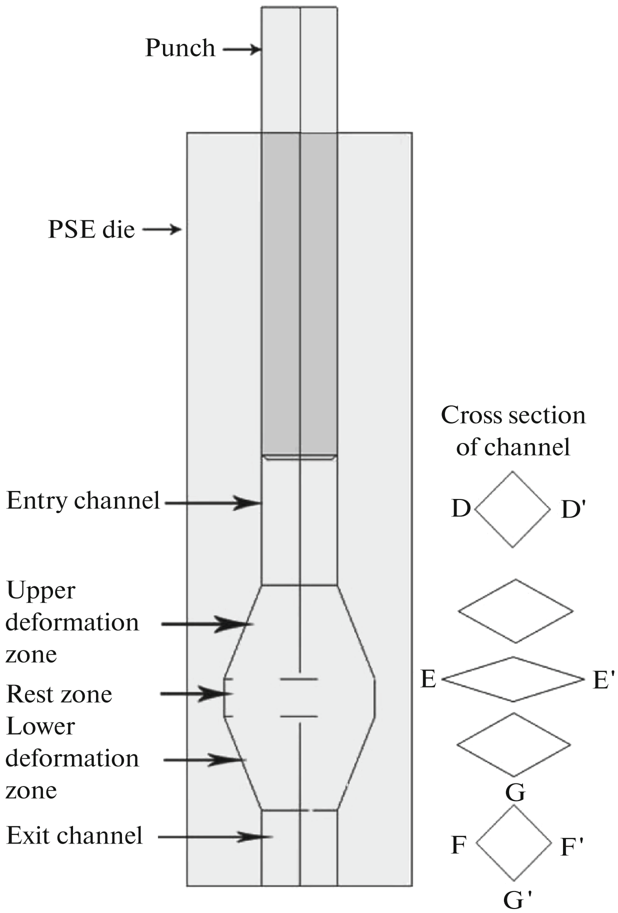

Fig. 1. Schematic diagram of pure shear extrusion process (left); gradual variation of the cross-sectional shape through the dies (right).

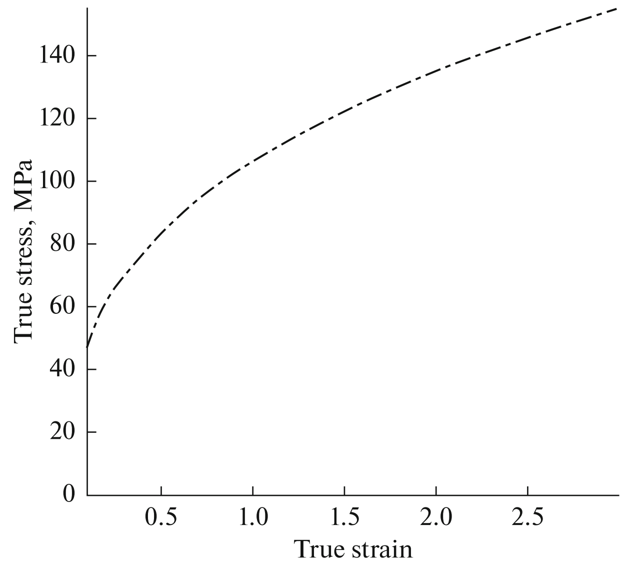

Fig. 2. Flow stress of AA1050 aluminum alloy.

increase in percentage of filling the exit channel with material, as reported by Yoon et al. [13].

In this paper, incomplete filling and strain inhomogeneity in a PSE process, which is a novel SPD method used to apply plastic deformation under pure shear condition, are studied [9, 17]. The PSE process has the potential to produce nanostructured materials with more homogeneous distribution of nano-sized grains. However, the process is not efficient, due to the incomplete filling of the exit channel. Therefore, in the present study, the effect of back pressure on the filling of exit channel by the material as well as strain homogeneity of deformed billet are studied in PSE using finite element method. A suitable value for back pressure is also recommended, which maximizes the filling fraction and strain average.

2. MATERIAL AND METHOD

A pure shear extrusion die is schematically shown in Fig. 1. The shear deformation is imposed at upper and lower deformation zones where the initial square cross section of the sample becomes rhombic and then changes back into a square while the cross-sectional area is constant. It is claimed that the rest zone where no deformation is imposed on the sample may improve filling fraction of the exit channel and homogeneity of strain [9].

The cross-sectional variation is also illustrated in Fig. 1. The ratio of the long diagonal of the rhombic ($\overline{EE'}$) to the diagonal of the initial square ($\overline{DD'}$) determines the amount of strain imposed on the billet, which is calculated as [9]:

$$\varepsilon_{eq} = \frac{4}{\sqrt{3}}\ln\left(\frac{\overline{EE'}}{\overline{DD'}}\right). \quad (1)$$

The ratio of $\frac{\overline{EE'}}{\overline{DD'}} = 2$ is applied in the PSE process modeled in this paper. Both the heights of the upper and lower deformation zones are equal to 25 mm, and the rest zone with a height of 10 mm is located between two deformation zones.

An AA1050 aluminum alloy billet with a square cross-section of 20 × 20 mm and length of 120 mm was used as the initial specimen in modeling. The cross-section of the model specimen was the same size as the cross-section of both the entry and exit channels of the PSE die.

A three dimensional finite element analysis of single pass PSE without back pressure was conducted using a general purpose metal forming simulator AFDEX 3D [18, 19]. The PSE die and punch were assumed to be rigid bodies. A constant punch speed of 1 mm/s was applied because of rate-independence of the AA1050 aluminum alloy of which flow curve is shown in Fig. 2 [12]. Adaptive meshing and automatic remeshing were made during the simulations. The

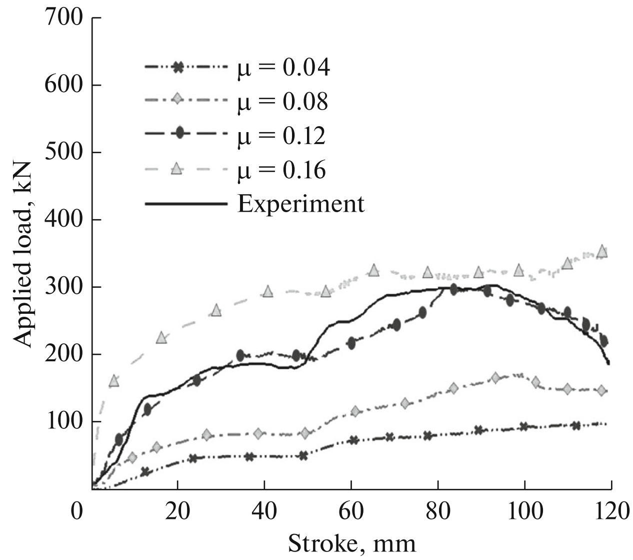

Fig. 3. Variation of applied load with stroke of punch.

simulations were carried out for various coefficients of Coulomb friction, μ, i.e., 0.04, 0.08, 0.12 and 0.16 to determine an optimized coefficient in term of forming load compared with experimental results of pure shear extrusion reported by Rahimi et al. [3, 20].

3. RESULTS AND DISCUSSION

3.1. Validation of Simulation

Comparison between the predictions and experiments were made from the standpoint of applied load and filling fraction. Figure 3 shows the variation of applied load with the stroke of punch. It is clearly seen that an acceptable agreement between the predictions and experiments of forming load is achieved at $\mu = 0.12$. In order to be sure about simulation accuracy, filling of exit channel was also investigated as the second criterion. Table 1 compares the predicted filling fraction of the cross-section at the exit channel for $\mu = 0.04$, 0.08, 0.12 and 0.16 with the experiment, revealing that the filling fraction predicted with $\mu = 0.12$ is the nearest to the experimental filling fraction of 91% [17]. It is apparent from the results that increase in the coefficient of friction leads increase in the filling fraction of the exit channel which inherently causes increase in forming load, i.e., reaction force against the metal flow in PSE process. This force plays the role of a kind of back pressure and pushes back the material to increasingly fill the exit channel of the die, implying that back pressure in this process increases the fraction of filling the cavity with material and thus leads to higher filling fraction.

3.2. Effects of Back Pressure on Filling Fraction and Strain

The effect of back pressure on filling fraction and strain homogeneity were studied using the same finite element model with $\mu = 0.12$ and a plunger attached at the beginning of the exit channel. Finite element analysis were conducted for the back pressures of 0, 100 and 200 MPa.

3.2.1. Filling fraction. Figure 4 illustrates the effects of back pressure on the material filling. As depicted in Fig. 4a, in PSE without back pressure, the material enters the exit channel with some cavities left.

In an effort to apply a higher shear stress on the material and to increase the filling fraction, the plunger was located as demonstrated in Fig. 4b. It was clear that the backward pressure against the material flow makes the material fill the deformation zones. Effect of back pressure on the metal flow lines of deformed material is also illustrated in Fig. 4.

The effect of back pressure on the material filling of the exit channel is illustrated in Fig. 5. As indicated, the unfilled volumes (white areas) are reducing with increase in back pressure from 0 to 200 MPa.

Figure 6 exhibits the variation of the predicted forming load with the stroke of punch in the presence of back pressure. It can be seen that the forming loads are almost the same at the primary stages of the processes, however, imposing the back pressure increases the final forming load. The comparison between the applied load curves without back pressure and with a back pressure of 200 MPa shows about 50% increase in the final forming load by the back pressure.

Table 1. The predicted filling fractions of the cross-section of the exit channel at various μ

Cross-section of extrusion in exit channel		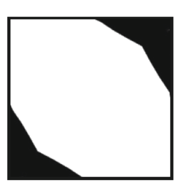	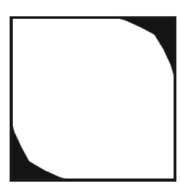	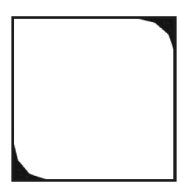	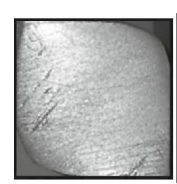
μ	0.04	0.08	0.12	0.16	Experiment
Filling fraction (%)	76.3	81.6	91.2	95.7	91

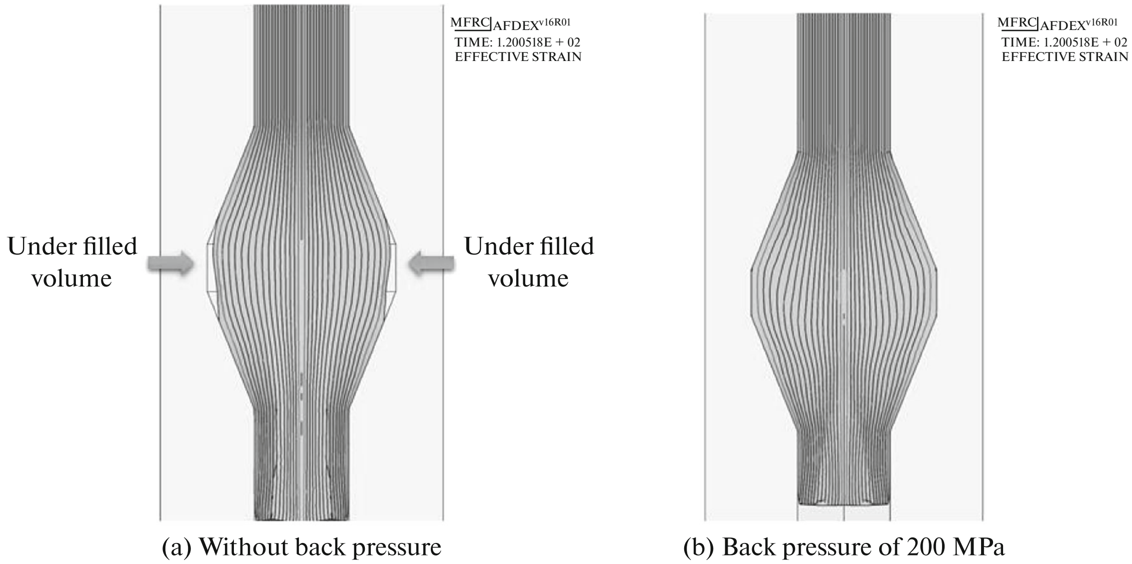

Fig. 4. Effect of back pressure on filling of deformation cavity.

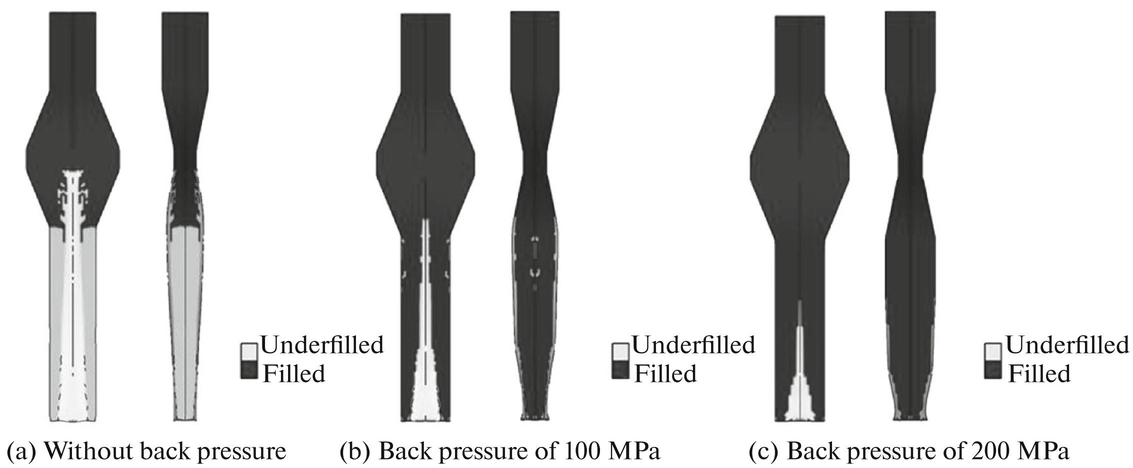

Fig. 5. Effect of back pressure on the predicted filling fraction of the exit channel (front and side views).

3.2.2. Effective strain. Figure 7 depicts the metal flow line of extruded billet in exit channel. The parallel flow lines at the entry of the channel show the steady state extrusion, which provides stable effective strain contours on the cross-section at the entry of the channel for the all cases.

Figures 8 and 9 depict the predicted effective strain of the PSE processed materials with various back pressures. The effective strain contours in the deformation cavity on the long diagonal of the rhombic cross-section are presented in Fig. 8. As explained earlier, when the billet passes through the upper and lower die zones, the material spreads in one diagonal while shrinking in the other one, i.e., the initial square cross-section becomes rhombic, and vice versa subsequently (see Fig. 1). Figure 8 shows the homogeneity of strain in the deformation zones reduces as back pressure increases. The trend toward lower homogeneity in the deformation zone shows that less homoge-

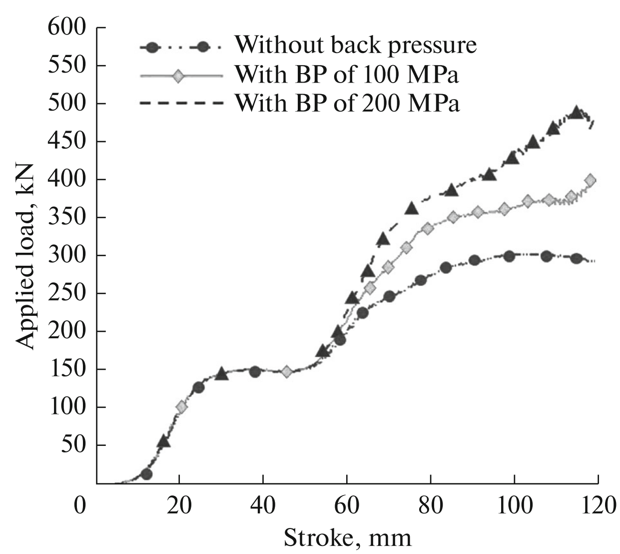

Fig. 6. Variation of predicted forming load with stroke of punch for various back pressure.

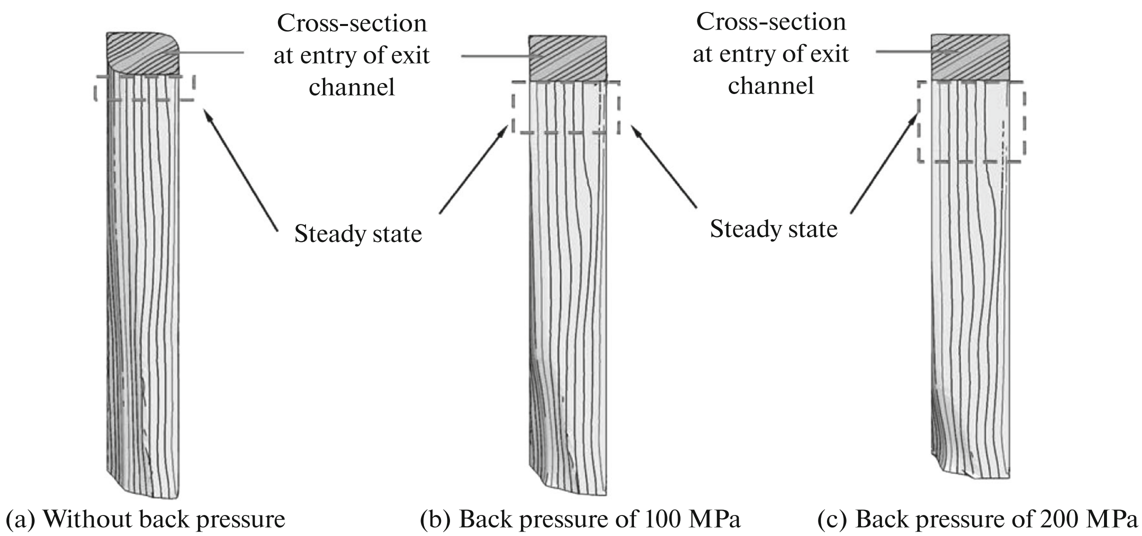

Fig. 7. Metal flow lines of exit channel.

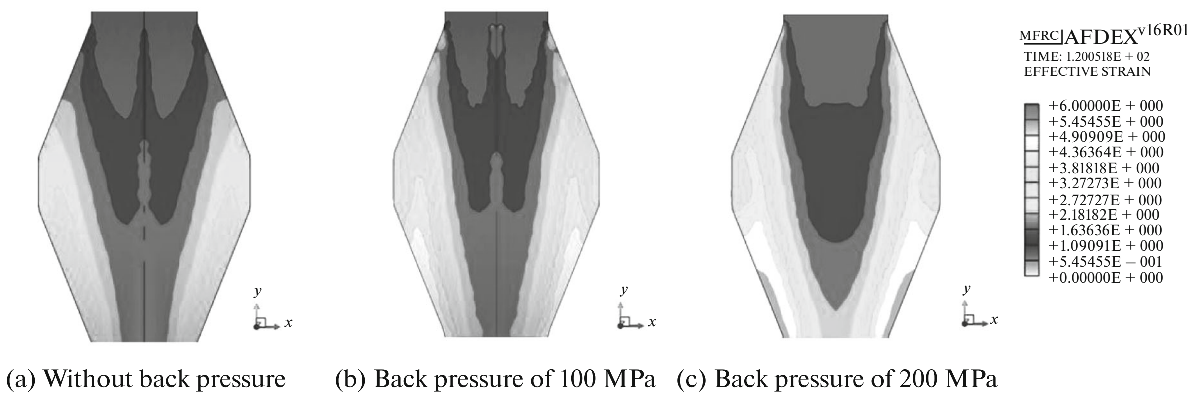

Fig. 8. Predicted effective strains in the die cavity of the PSE process.

neous effective strain in the PSE product is expected when back pressure is applied.

Figure 9 shows the distribution of effective strain on cross-sections at the entry of the exit channel. It is clear that the sharp corners contain the largest strains due to the friction at the die-material interface where severe plastic deformation is experienced. The gap between the die and material at the round corners is diminished as the back pressure increases, which meets well with previous discussions about the filling fraction of the exit channel. Moreover, the homogeneity of the effective strain is deteriorated slightly with higher back pressure, as indicated in Fig. 9c.

For comparing the results of strain distribution on the cross-section at the entry of exit channel, the variation of the effective strain along FF' and GG', the diagonals of cross-section determined in Fig. 1, is plotted in Fig. 10. As can be seen in Fig. 10a, a higher strain at the periphery of the material along FF' is observed in the curve related to the PSE with 200 MPa back pressure. On the other side, in Fig. 10b, the distribution of effective strain along GG' shows less heterogeneity compared to the FF'. Despite variation of strain homogeneity along FF', the strain homogeneity along GG' is improved as the back pressure increased.

In order to obtain quantitative information regarding the strain homogeneity, the strain inhomogeneity index is defined as follows [21]:

$$C_{\mathrm{i}} = \frac{\bar{\varepsilon}_{\max} - \bar{\varepsilon}_{\min}}{\bar{\varepsilon}_{\mathrm{ave}}}, \qquad (2)$$

where $\bar{\varepsilon}_{\max}$, $\bar{\varepsilon}_{\min}$ and $\bar{\varepsilon}_{\mathrm{ave}}$ are the maximum, minimum and average magnitudes of effective strain, respectively. The amount of average effective strain and strain inhomogeneity index, C_{i}, at different back pressures are shown in Fig. 11, indicating that the average of the effective strain increases from 2.1 in a PSE without back pressure to 2.5 at the back pressure of

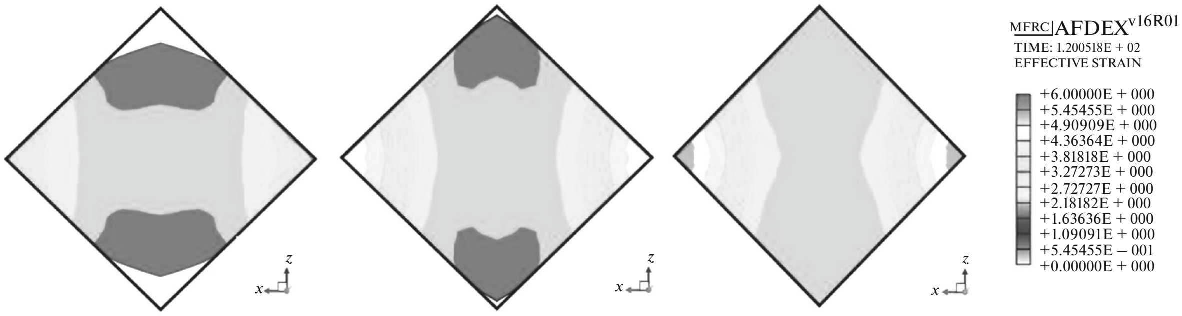

(a) Without back pressure (b) Back pressure of 100 MPa (c) Back pressure of 200 MPa

Fig. 9. Predicted effective strains on a cross-section at the entry of the exit channel.

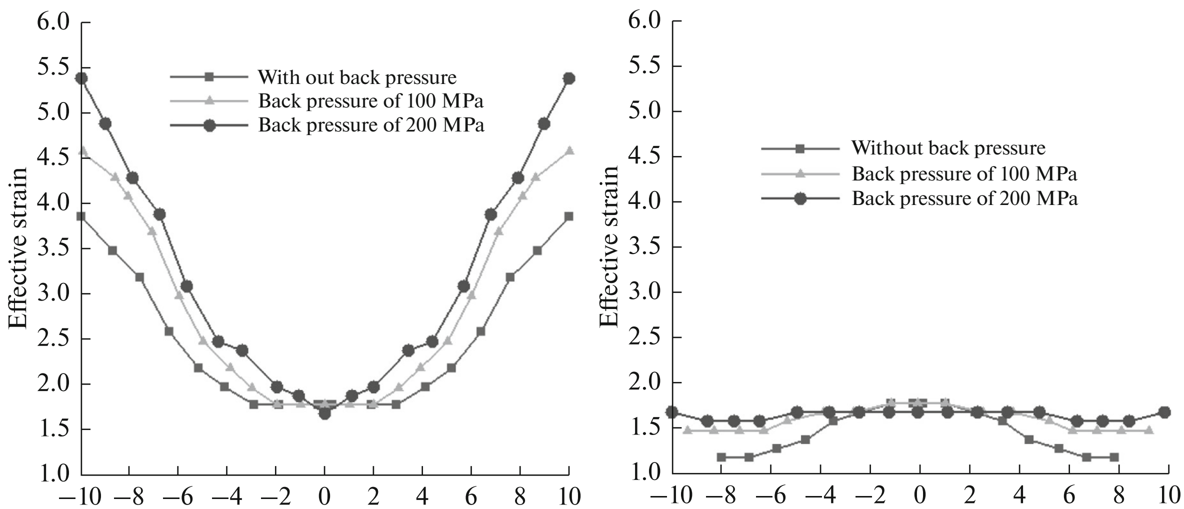

(a) Along the FF' diagonal (b) Along the GG' diagonal

Fig. 10. Effect of back pressure on strain distribution along the diagonals of cross-section at the entry of exit channel.

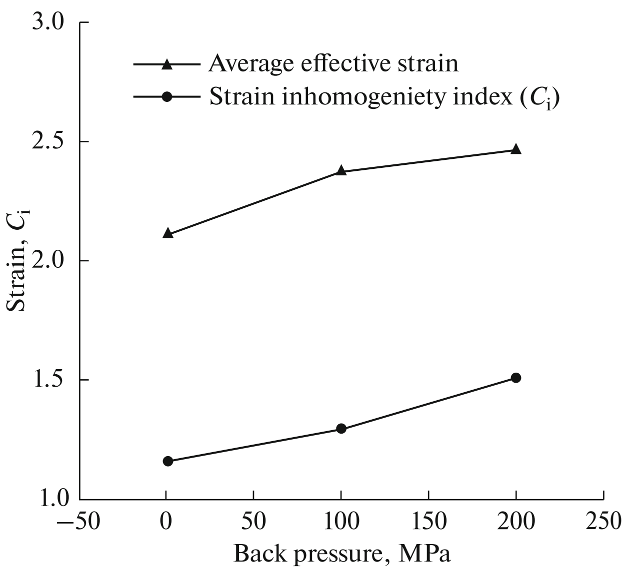

Fig. 11. Effect of BP on the average effective strain and strain inhomogeneity index (C_i).

200 MPa. Meanwhile, the strain inhomogeneity index increases from 1.2 to 1.5 as the back pressure increases.

4. CONCLUSIONS

In this study, we investigated the effects of back pressure on PSE using finite element method. In order to determine the key parameters of process i.e., coefficient of Coulomb friction and flow stress, first a PSE process without back pressure from the literature was simulated with various Coulomb friction factors using a specified flow stress curve from the literature and an acceptable agreement between the predictions and experiments of forming load and filled fraction of exit channel is achieved at $\mu = 0.12$.

Afterward, the effect of back pressure on the filling fraction of exit channel and the strain homogeneity of PSEed material were studied through simulating the process at $\mu = 0.12$. For this purpose, a plunger was located at the entry of exit channel to apply the back pressure.

The results showed that back pressure increases the filled fraction of the exit channel and magnitude of applied strain but it reduces homogeneity of effective strain. The prediction of strain distribution on the cross-section of exit channel revealed that the homogeneity of the effective strain is reduced slightly with higher back pressure. In a quantitative view, the average effective strain and the strain inhomogeneity index increase 19% and 25% respectively as the back pressure increases. Since according to the literature, PSE induces more homogeneous strain compared to the others SPD processes by itself, the PSE with back pressure produces a severe plastic deformed material with higher magnitude of strain and less strain homogeneity.

ACKNOWLEDGMENTS

This work is supported by the BK 21 plus project, the project for industry-university cooperative research of the Korean Small and Medium Business Administration and World Class 300.

REFERENCES

1. Mohammadi, S., Irani, M., and Karimi Taheri, A., *Russ. J. Non-Ferrous Met.*, 2015, vol. 56, pp. 206–211.
2. Bhargava, S., Nigam, V., Arora, K., Sahai, A., and Sharma, R.S., *Proc. Mater. Sci.*, 2014, vol. 5, pp. 719–725.
3. Rahimi, F., Eivani, A.R., and Kiani, M., *Mater. Des.*, 2015, vol. 83, pp. 144–153.
4. Deng, G., Lu, C., Su, L., Tieu, A.K., Li, J., Liu, M., Zhu, H., and Liu, X., *Comp. Mater. Sci.*, 2014, vol. 81, pp. 79–88.
5. Kim, H.S., Seo, M.H., and Hong, S.I., *J. Mater. Proc. Technol.*, 2001, vol. 113, p. 622.
6. Kawasaki, M., Figueiredo, R.B., and Langdon, T.G., *J. Mater. Sci.*, 2012, vol. 47, p. 7719.
7. Dunne, F.P.E., *Int. J. Plast.*, 1998, vol. 14, p. 413.
8. Haghdadi, N., Zarei-Hanzaki, A., Abou-Ras, D., Maghsoudi, M.H., and Ghorbani, A., *Mater. Sci. Eng. A*, 2014, vol. 595, pp. 179–187.
9. Eivani, A.R., *Mater. Lett.*, 2015, vol. 139, pp. 15–18.
10. Son, I.H., Lee, J.H., and Im, Y.T., *J. Mater. Proc. Technol.*, 2006, vol. 171, pp. 480–487.
11. Mckenzie, P.W.J., Lapovok, R., Estrin, Y., *Acta Mater.*, 2007, vol. 55, pp. 2985–2993.
12. Kim, J.G., Latypov, M., Pardis, N., Beygelzimer, Y.E., and Kim, H.S., *Mater. Des.*, 2015, vol. 83, pp. 858–865.
13. Yoon, S.C., Jeong, H.G., Lee, S., and Kim, H.S., *Comp. Mater. Sci.*, 2013, vol. 77, pp. 202–207.
14. Oh, S.J. and Kang, S.B., *Mater. Sci. Eng. A*, 2003, vol. 343, pp. 107–115.
15. Akbari Mousavi, S.A.A., Bahadori, S.R., and Shahab, A.R., *Mater. Sci. Eng. A*, 2010, vol. 527, pp. 3967–3974.
16. Kawasaki, M., Figueiredo, R.B., and Langdon, T.G., *Acta Mater.*, 2011, vol. 59, pp. 308–316.
17. Rahimi, F. and Eivani, A.R., *Mater. Sci. Eng. A*, 2015, vol. 626, pp. 423–431.
18. Lee, M.C., Chung, S.H., Jang, S.M., and Joun, M.S., *Finite. Elem. Anal. Des.*, 2009, vol. 45, pp. 745–754.
19. ManSoo Joun, Jea Gun Eom, and Min Cheol Lee, *Mech. Mater.*, 2008, vol. 40, pp. 586–593.
20. Joun, M.S., Moon, H.G., Choi, I.S., Lee, M.C., and Jun, B.Y., *Tribol. Int.*, 2009, vol. 42, pp. 311–319.
21. Djavanroodi, F., Daneshtalab, M., and Ebrahimi, M., *Mater. Sci. Eng. A*, 2012, vol. 535, pp. 115–121.